




A New Method for Imaging Seismic Quiescence and Its Application to the $M_w = 8.3$ Kurile Islands Earthquake on 15 November 2006

KEI KATSUMATA¹  and JIANCANG ZHUANG²

Abstract—In the present paper, a new method referred to as the Poisson probability map (PMAP) method is presented for identifying and visualizing seismic quiescence. With the PMAP, the P -value is defined as the probability that consecutive earthquakes occur according to a homogeneous Poisson process: the smaller the P -value, the less frequently the longer time interval is observed, i.e. the more significant the seismic quiescence. The PMAP method was applied to the sequence which preceded the Kurile Islands earthquake that occurred on 15 November 2006 [$M_w = 8.3$ and the centroid = (154.33 °E, 46.71 °N)]. The seismic quiescence is identified by a small P -value of 9.0×10^{-5} that was found to start in 1990.1, which lasted for 15.4 years and ended in 2005.5 within a circular area centered at (153.8 °E, 47.1 °N) and with a radius of 26 km. This seismic quiescence has not previously been recognized using any other method.

Keywords: Seismic quiescence, seismicity, Poisson probability map (PMAP), ZMAP, Kurile Islands earthquake.

1. Introduction

The seismic quiescence hypothesis is an empirical model in which the number of small earthquakes decreases in and around the assumed focal area of a great earthquake when its occurrence time is approaching (e.g., Inouye 1965; Utsu 1968; Mogi 1969; Kelleher and Savino 1975; Ohtake et al. 1977; Ogata 1992). Discussion continues as to whether this hypothesis is correct, and therefore additional case studies are required. Various methods have been

proposed to investigate seismic quiescence, including the RTL method (Sobolev and Tyupkin 1997; Huang 2004; Gentilia et al. 2019) and the ZMAP method (Wiemer and Wyss 1994). The ZMAP method is a statistical technique for systematically searching for spatial and temporal changes in seismicity. For a more specific explanation of the ZMAP method, see Wiemer and Wyss (1994) and Katsumata (2011). Since the ZMAP computer program has a rich graphical user interface and is very easy to operate, it has been commonly used to investigate the seismic quiescence that occurs before large earthquakes (e.g., Wyss et al. 1999; Wu and Chiao 2006; Katsumata 2011). In the ZMAP method, a study area is divided into a grid, N earthquakes are selected around each node, and the Z -value is calculated using the following equation:

$$Z = (R_{bg} - R_w) / (S_{bg}/n_{bg} + S_w/n_w)^{1/2}, \quad (1)$$

where R_{bg} and R_w are the occurrence rates for background earthquakes and those occurring in a time window T_w , respectively, S_{bg} and n_{bg} are the variance and the number of bins in the background period, respectively, and S_w and n_w are the variance and the number of bins in time window T_w , respectively. A simple example of the calculation of the Z -value is described in supplementary material 1. Note that large positive Z -values correspond to a decrease in the seismicity rate.

A great earthquake occurred on 15 November 2006 in the central Kurile Islands region. The centroid moment tensor (CMT) solution for this earthquake was determined by the Global CMT project (Dziewonski et al. 1981; Ekström et al. 2012; available at <https://www.globalcmt.org/CMTsearch.html>). The centroid was located at 46.71 °N and

Electronic supplementary material The online version of this article (<https://doi.org/10.1007/s00024-020-02498-w>) contains supplementary material, which is available to authorized users.

¹ Institute of Seismology and Volcanology, Faculty of Science, Hokkaido University, Sapporo 060-0810, Japan. E-mail: kkatsu@sci.hokudai.ac.jp

² Institute of Statistical Mathematics, 10-3 Midori-cho, Tachikawa, Tokyo 190-8562, Japan.

154.33 °E at a depth of 13.5 km. The seismic moment was 3.51×10^{21} Nm ($M_w = 8.3$), and the fault plane was (strike, dip, slip) = (215°, 15°, 92°). This event was a low-angle megathrust interplate earthquake on the upper surface of the Pacific Plate subducting beneath the North American or the Okhotsk Sea Plate (e.g., Seno et al. 1996; Takahashi et al. 1999). This great earthquake filled the southwestern half of a seismic gap (Fedotov 1968; Kelleher and McCann 1976; McCann et al. 1979; Nishenko 1991). This seismic gap is located along the Kurile Trench between the great 1963 Kuril Islands ($M_w = 8.5$) earthquake (Kanamori 1970; Beck and Ruff 1987) and the great 1952 Kamchatka ($M_w = 9.0$) earthquake (Kanamori 1976; Johnson and Satake 1999).

Although Katsumata (2017) investigated the seismicity in and around the Japan subduction zone from 1975 to 2012 in order to search for the long-term seismic quiescence preceding great earthquakes using the ZMAP method, no seismic quiescence was detected before the 2006 Kurile Islands earthquake. The reasons for this oversight appeared to be due to the following issues with the ZMAP method: (1) When no earthquake is observed in a time window T_w , i.e. $R_w = S_w = 0$, the Z -value is approximately the same whether T_w is long or short. (2) The length of the time window T_w is arbitrary and must be empirically assumed. (3) The number N of earthquakes around each node is also arbitrary and is the same for all nodes. In order to address these issues, a new method is presented herein. The new method calculates the probability that no earthquake will occur. The longer the period when the earthquake does not occur, the smaller the probability; therefore, it becomes a measure of seismic quiescence. The proposed method is applied to the $M_w = 8.3$ Kurile Islands earthquake on 15 November 2006, and the suitability of the proposed method is discussed.

2. Data

An earthquake catalog compiled by the International Seismological Center (ISC) (International Seismological Center 2013) was used to investigate the seismicity in and around the focal area of the 2006 Kurile Islands earthquake. The study area was

defined by the circle of investigation (CI) used in the M8 algorithm (Keilis-Borok and Kossobokov 1990). The diameter of the CI was calculated using $D = \exp(M_w - 5.6) + 1.0 = 15.88^\circ$ for a meridian length of 1763 km (Fig. 1). The center of the CI was located at the centroid of the main shock, and earthquakes within a radius of 882 km were downloaded from the Reviewed ISC Bulletin (<ftp://isc-mirror.iris.washington.edu/pub/ffb/catalogue/>). Although the ISC has finished rebuilding the bulletin from 1964 to 1979 (Storchak et al. 2017), old data stored in the “prerebuild” directory (<ftp://isc-mirror.iris.washington.edu/pub/prerebuild/ffb/catalogue/>) were used in the present study to maintain the temporal homogeneity of the earthquake catalog. Earthquakes satisfying the following three conditions were selected: (1) the earthquake occurred between 1 January 1964 and 14 November 2006, (2) the body wave magnitude was $m_b \geq M_C$, and (3) the depth of the hypocenter was ≤ 60 km. Here, M_C is the minimum magnitude of completeness, and the number of earthquakes versus magnitude was examined for the catalog in order to estimate M_C . In the present study, M_C is defined as the magnitude for which at least 90% of the frequency-magnitude distribution can be modeled using a power law (Wiemer and Wyss 2000). The result indicated that M_C ranged from 4.2 to 4.7, depending on the period. Figure 2 shows a temporal change in M_C . In general, M_C fluctuates in time due to slight changes in observational conditions, such as installation of new seismic stations, closing of old seismic stations, temporary interruption in observation, or changes in the combination of seismic stations used for magnitude calculation. Taking the fluctuation into account, M_C was set to be 5.0 in the present study. Consequently, the number of earthquakes with $m_b \geq M_C$ was 2239 within the CI (Fig. 1 and supplementary material 2).

Seismicity typically comprises two kinds of activity: background activity and cluster activity. Aftershocks and earthquake swarms are typical of cluster activity. In the present study, the temporal change in background activity was investigated in order to search for seismic quiescence before the 2006 Kurile Islands earthquake, and thus the cluster activity was removed from the ISC catalog using a stochastic declustering method (Zhuang et al. 2005),

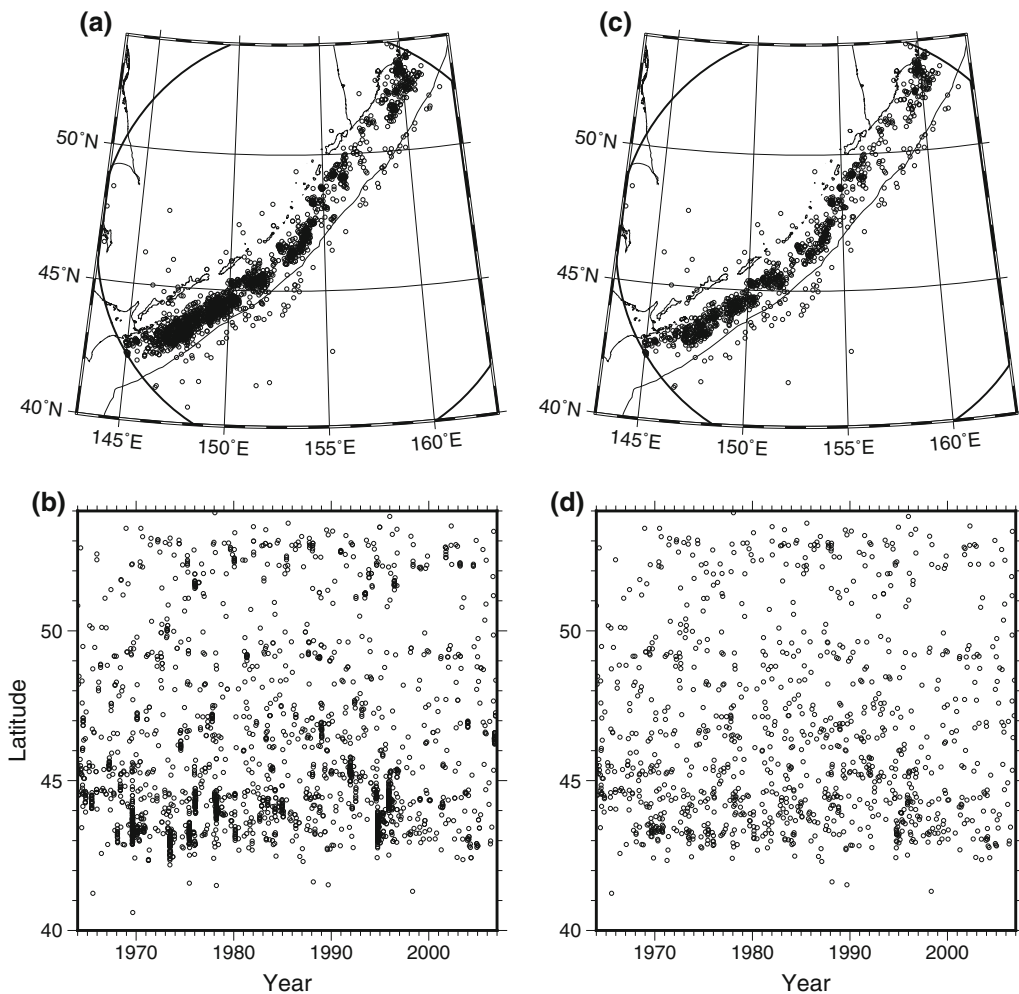


Figure 1

Earthquakes considered in the present study. **a** and **c** Earthquake distributions before and after the declustering process, respectively. Each earthquake list is provided in supplementary material 2 and 3. Earthquakes were selected from the ISC catalog and occurred from 1 January 1964 to 14 November 2006, with $m_b \geq 5.0$ and depth ≤ 60 km. The large circle is the circle of investigation (CI), and the solid line along the Kurile Islands indicates the plate boundary (Bird 2003). **b** and **d** Space-time plots before and after the declustering process, respectively

which is based on an epidemic-type aftershock sequence (ETAS) model (Ogata 1988, 2004). The ETAS parameters in model 5 of Zhuang et al. (2005) were determined as follows: $A = 0.330$, $\alpha = 1.58$, $c = 0.0177$, $p = 1.217$, $D^2 = 0.00827$, $q = 1.96$, and $\gamma = 1.21$. After the declustering process, 1096 earthquakes were identified as background seismicity and are the basis of the analyses in the present study (Fig. 1 and supplementary material 3). Although M_C fluctuates slightly in time, a cumulative number curve in Fig. 2 shows that the background seismicity rate is

almost constant for earthquakes with $M = 5.0$ and larger.

3. Method

In order to search for a seismic quiescence, a rectangular area was defined to include the CI, i.e. $40\text{--}54^\circ\text{N}$ and $143\text{--}163^\circ\text{E}$. This area was divided into a grid with an interval of 0.1° in latitude by 0.1° in longitude. A circle centered on a node (x, y) was drawn with a radius of R [km], and R was increased

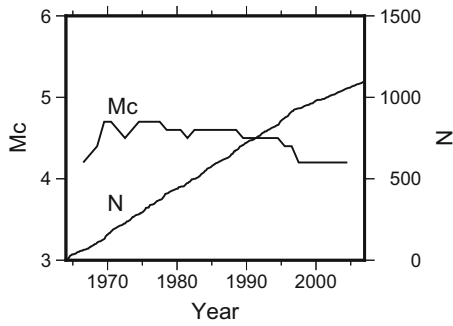


Figure 2

Temporal change in magnitude completeness (M_c) and the cumulative number of earthquakes evaluated as a background seismicity (N)

gradually so that the number of earthquakes was N within the circle. This circle is defined as the resolution circle, and the radius R is defined as the spatial resolution (Wiemer and Wyss 1994).

In order to resolve the issues with the ZMAP method, another parameter was introduced in the present study. First, we assume that earthquake occurrence follows a stationary Poisson process in time (e.g., Utsu 1969; Gardner and Knopoff 1974), and the average rate of occurrence μ is defined as:

$$\mu = \frac{N}{T} [(\text{number of earthquakes})/\text{year}] \quad (2)$$

where T is the observation time in years, and N is the number of earthquakes that occurred in the resolution circle during T . In this case, an average of λ earthquakes occur during dt years:

$$\lambda = \mu dt \quad (3)$$

Assuming that an average of λ earthquakes occur, the probability that n earthquakes occur during dt years is:

$$P(n) = \frac{\lambda^n e^{-\lambda}}{n!} \quad (4)$$

Therefore, the probability that no earthquake occurs during dt years, i.e. dt is the interval between earthquake occurrence, is obtained by substituting 0 for n in Eq. (4):

$$P(0) = \frac{\lambda^0 e^{-\lambda}}{0!} = e^{-\lambda} \quad (5)$$

In the present study, $P(0)$ in Eq. (5) is used to measure the seismic quiescence quantitatively. As mentioned above, there are N earthquakes within the resolution circle. Suppose that their origin times are $t_1, t_2, \dots, t_i, t_{i+1}, \dots, t_N$ in order of occurrence. Here, dt is defined at time t as follows:

$$dt = t - t_i (t_i \leq t < t_{i+1}) \quad (6)$$

In this case, $P(0)$ is obtained as follows:

$$P_N(0) = \exp\left\{-\frac{N}{T}(t - t_i)\right\} \quad (7)$$

where $P_N(0)$ is a function of N ranging from 5 to 40 in the present study. Finally, the P -value is defined at node (x, y) at time t as:

$$P(x, y, t) = \min_{5 \leq N \leq 40} P_N(0) \quad (8)$$

where x ranges from 143 °E to 163 °E with an interval of 0.1 °, y ranges from 40 °N to 54 °N with an interval of 0.1°, and t ranges from 1964.8 to 2006.8 with an interval of 0.1 years. If the spatial resolution R is larger than 50 km for all N values at a node, then the P -value was not calculated at the node. The smaller the P -value, the more significant the seismic quiescence.

A simple example of the P -value calculation is as follows. Suppose that this is an earthquake catalog from 1964.0 to 2007.0, i.e. 43.0 years, and a time slice is produced at time $t = 2000.0$. First, $N = 15$ earthquakes are selected around a spatial node, and they are arranged from oldest earthquakes in chronological order (Fig. 3a). Let the occurrence times of these 15 earthquakes be t_1, t_2, \dots, t_{15} . The value of i that satisfies the condition $t_i < t < t_{i+1}$ is $i = 12$, i.e. $t_{12} = 1990.137$ and $t_{13} = 2005.581$. In this example, $dt = t - t_{12} = 2000.0 - 1990.137 = 9.863$ years. The average rate of occurrence is $\mu = 15/43.0 = 0.3488$ events/year, $\lambda = \mu dt = 0.3488 \times 9.863 = 3.440$, and thus $P(0) = \exp(-\lambda) = \exp(-3.440) = 0.0321$. Second, $N = 28$ earthquakes are selected around the node (Fig. 3b). The value of i that satisfies the condition $t_i < t < t_{i+1}$ is $i = 25$, i.e. $t_{25} = 1990.137$ and $t_{26} = 2005.581$, $dt = t - t_{25} = 2000.0 - 1990.137 = 9.863$ years, $\mu = 28/43.0 = 0.6512$ events/year, $\lambda = \mu dt = 0.6512 \times 9.863 = 6.423$, and

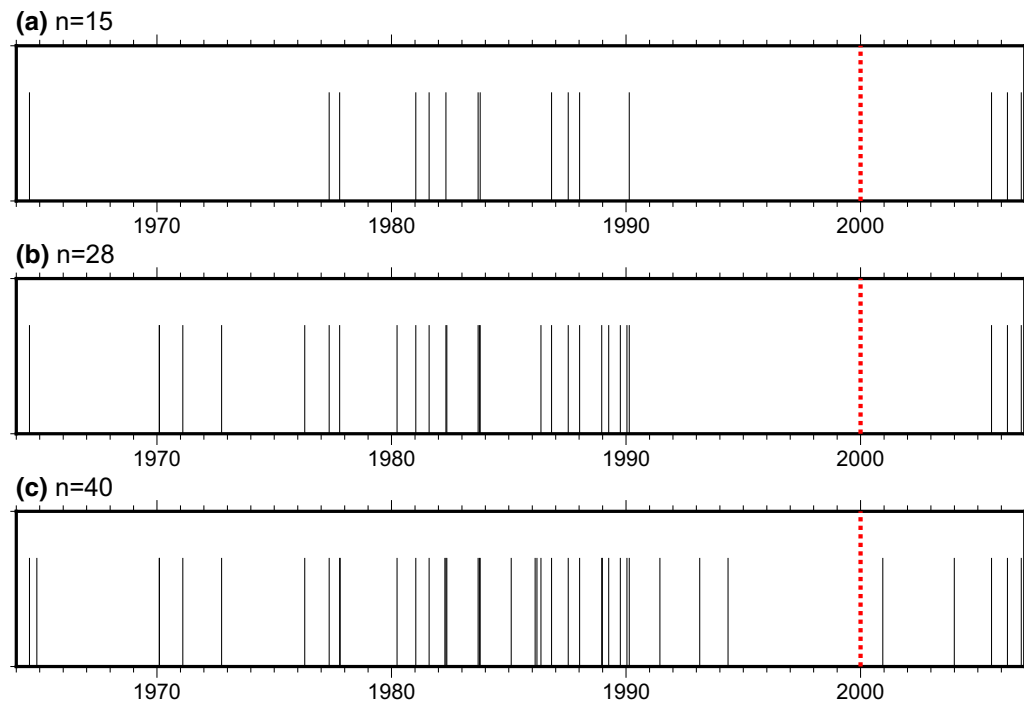


Figure 3

Time series of earthquakes from 1964 to 2006. **a** $n = 15$, **b** $n = 28$, and **c** $n = 40$ earthquakes were selected around a node. A red vertical dashed line indicates the time that the P -value is calculated

thus $P(0) = \exp(-\lambda) = \exp(-6.423) = 0.00162$. Finally, $N = 40$ earthquakes are selected around the node (Fig. 3c). The value of i that satisfies the condition $t_i < t < t_{i+1}$ is $i = 35$, i.e. $t_{35} = 1994.351$ and $t_{36} = 2000.948$, $dt = t - t_{35} = 2000.0 - 1994.351 = 5.649$ years, $\mu = 40/43.0 = 0.9302$ events/year, $\lambda = \mu dt = 0.9302 \times 5.649 = 5.255$, and thus $P(0) = \exp(-\lambda) = \exp(-5.255) = 0.00522$. In the above example, we supposed a time slice at $t = 2000.0$ and N took three values: 15, 28, and 40. As a result, the $P(0)$ becomes the minimum when $N = 28$. At this spatial node, the minimum value, i.e. $P(0) = 0.00162$, is defined as the P -value at the time $t = 2000.0$. In actual analysis, N increases from 5 to 40 by 1 for finding the smallest $P(0)$ at each node. Moreover, the time t increases from 1964.8 to 2006.8 by 0.1 years. Using the above method, we were able to create a P -value spatial map every 0.1 year.

4. Results

As in the ZMAP method, the temporal change in the P -value was visualized. One frame of time was produced and displayed every 0.1 year, and the frames were used to visualize small P -values (Fig. 4 and supplementary material 4). Note that the smaller the P -value, the more significant the seismic quiescence. These visual time slices are called a Poisson probability map (PMAP) in the present study. By investigating all frames of time using PMAP, a node with a very small P -value was found in the focal area of the 2006 Kurile Islands earthquake. The parameters are as follows: $x = 153.8$ °E, $y = 47.1$ °N, $t = 2005.5$, $N = 26$, $R = 26$ km, $dt = 15.4$ years, and $P = 9.0 \times 10^{-5}$ or $\log_{10}P = -4.05$. The P -value at this node is the smallest in and around the focal area of the 2006 earthquake between $t = 1964.8$ and 2006.8. The second smallest P -value was obtained for the following parameters: $x = 153.5$ °E, $y = 47.0$ °N,

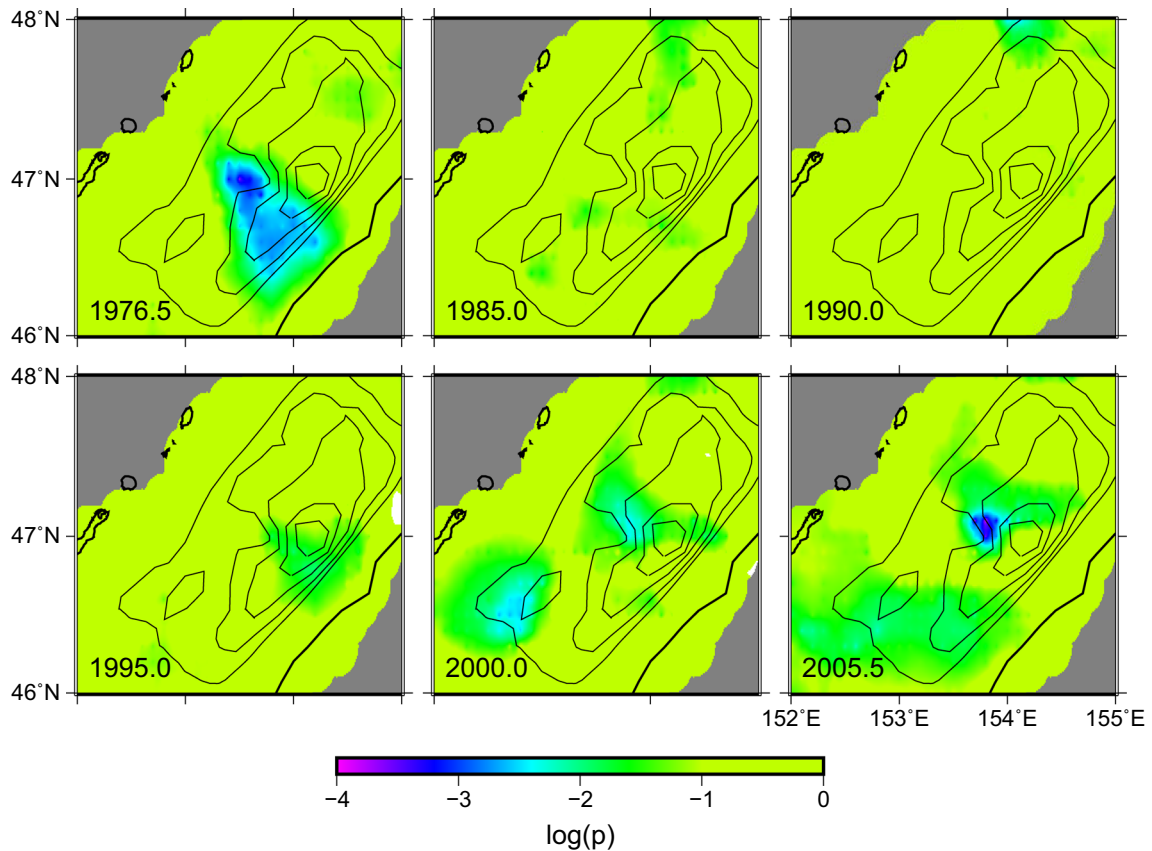


Figure 4

Time slices of the P -value distribution using the declustered ISC catalog. The time is indicated at the left bottom of each slice. All nodes are colored if the radius of the resolution circle is smaller than 50 km. The smaller the P -value, the more significant the seismic quiescence. The coseismic slip distribution model for the 2006 Kurile Islands earthquake is shown using contours of 1, 4, 7, 10, and 13 m (Lay et al. 2009). All time slices from 1964.8 to 2006.8 are shown at intervals of 0.1 year as a motion picture in supplementary material 4

$t = 1976.5$, $N = 33$, $R = 43$ km, $dt = 10.8$ years, and $P = 2.4 \times 10^{-4}$ or $\log_{10}P = -3.62$. Wyss and Habermann (1979) pointed out the seismic quiescence corresponding to the second smallest P -value at $t = 1976.5$. Interestingly, the smallest and second smallest P -values were located very close to each other in space. However, they were separated by 29 years. This strongly suggests that not all seismic quiescence leads to a subsequent great earthquake.

The seismic quiescence at $t = 2005.5$ was investigated in detail (Fig. 5a). The node is located 59 km northwest of the centroid of the 2006 main shock. In the present study, the seismic quiescence area that suffered from a significant decrease in seismicity is defined as a circle centered at (x, y) with a radius of R . The seismic quiescence area is much smaller than

the focal area with a slip larger than 1 m during the main shock and is located close to the area with a slip larger than 10 m. This can be considered as an asperity with a large slip. If this is the case, the seismic quiescence area is strongly associated with the asperity that was ruptured by the subsequent main shock. The temporal features of the seismic quiescence found above are as follows (Fig. 5b). Twenty-three earthquakes occurred from 1964.0 to 1990.1, and thus the average occurrence rate was $23/26.1 = 0.88$ events/year. Although earthquakes occurred rather regularly during this period, since 1990.1, earthquakes have completely ceased to occur. The seismic quiescence started at $t = 1990.1$, and the duration was $dt = 15.4$ years (from 1990.1 to 2005.5). After 2005.5, three earthquakes occurred in

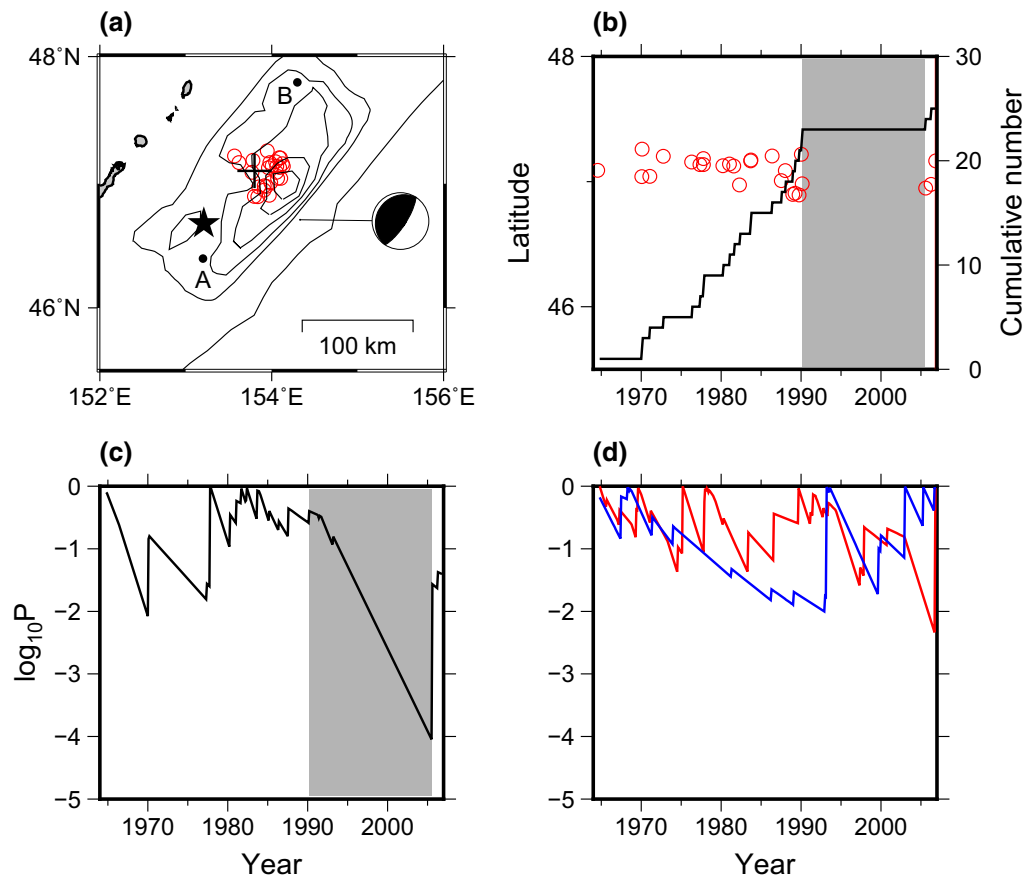


Figure 5

a The cross indicates the spatial node at the center of the seismic quiescence area. Red circles are epicenters selected around the node and are located within the seismic quiescence area. The black star indicates the epicenter of the main shock. The coseismic slip distribution model for the 2006 Kurile Islands earthquake is shown as contours of 1, 4, 7, 10, and 13 m (Lay et al. 2009). The plate boundary is shown by solid lines (Bird 2003). **b** Space–time plot (red circles) and cumulative number curve (black line) of the epicenters in (a). The time period for the seismic quiescence is shown in gray. **c** Change in P -value as a function of time at the node shown as the cross in (a). The time period of seismic quiescence is shown in gray. **d** Temporal change in P -value without seismic quiescence. Red and blue lines indicate temporal changes in P -values at nodes A and B in (a), respectively

the 1.3 years between 2005.5 and 2006.8. The $\log_{10}P$ -value ranged from -2 to 0 between 1964.8 and 1990.1, and after 1990.1, monotonically decreased to below -4 (Fig. 5c). The $\log_{10}P$ -value appears to fluctuate between -2 and 0 when earthquakes occur randomly without any long-term seismic quiescence (Fig. 5d). Compared to usual fluctuations of the P -value, the value of $\log_{10}P = -4.05$ is two orders of magnitude smaller.

5. Discussion

In the present study, a long-term seismic quiescence was found to be located very close to an asperity that was ruptured by the subsequent main shock of the 2006 Kurile Islands earthquake. As a measure of the rarity of the seismic quiescence, the P -value was introduced. The smaller the P -value, the rarer the occurrence of seismic quiescence. In this case, $P = 9.0 \times 10^{-5}$ or $\log_{10}P = -4.05$ is the smallest value in and around the focal area. Although Katsumata (2017) failed to detect seismic quiescence before the 2006 Kurile Islands earthquake using the

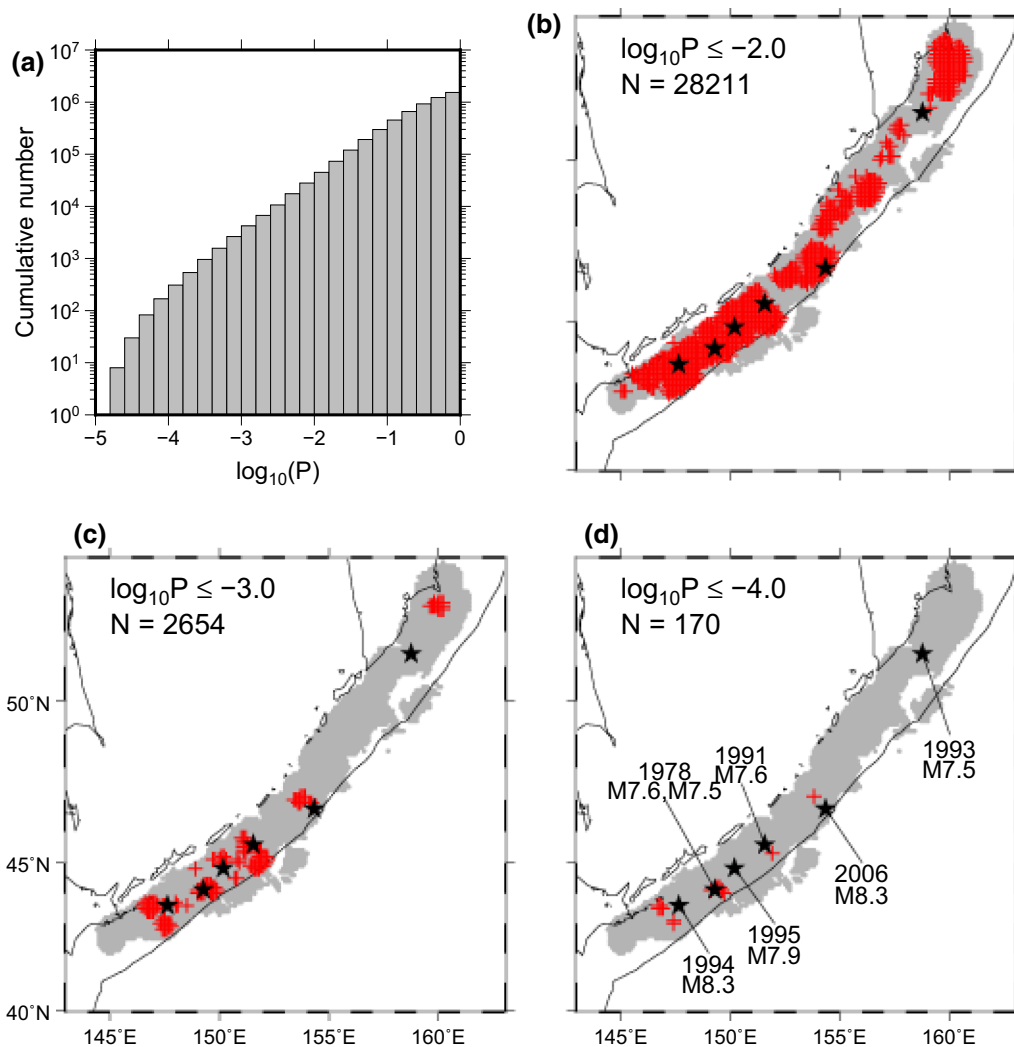


Figure 6

a Cumulative number of P -values calculated in the entire study area. **b** Red crosses show nodes with $\log_{10}P \leq -2.0$ from 1964.8 to 2006.8. Closed stars indicate earthquakes that occurred within the CI with $M_w \geq 7.5$ with a centroid at a depth ≤ 100 km listed on the Global CMT catalog from 1976 to 2006. The P -value was calculated at nodes in the gray area. The plate boundary is shown by solid lines (Bird 2003). **c** and **d** Distribution of nodes with $\log_{10}P \leq -3.0$ and $\log_{10}P \leq -4.0$, respectively

ZMAP method, the seismic quiescence 16.7 years before the 2006 earthquake was successfully detected using the PMAP method in the present study.

The next problem to consider is how frequently such small P -values are observed. The P -value was obtained at 3657 spatial nodes within the study area and at 421 temporal nodes between 1964.8 and 2006.8. Thus, the total number of P -values calculated is $3657 \times 421 = 1,539,597$. Note that the P -values are not independent from each other. Since the distance between neighboring nodes are 0.1° , their

resolution circles are partly overlapped, and the same earthquakes are sampled. The P -value ranged from 1.6×10^{-5} to 1.0, i.e. $-4.8 \leq \log_{10}P \leq 0$, in the entire study area (Fig. 6a). The number of P -values less than or equal to 1.0×10^{-4} is 170, which is 0.01% of the total number. The spatial distributions of the nodes are shown for $\log_{10}P \leq -2.0$, -3.0 , and -4.0 in Fig. 6b, c, and d, respectively. These nodes appear to be clustered rather than scattered uniformly along the Kurile Trench. When $\log_{10}P \leq -4.0$, the 170 nodes are clearly divided into four groups. The

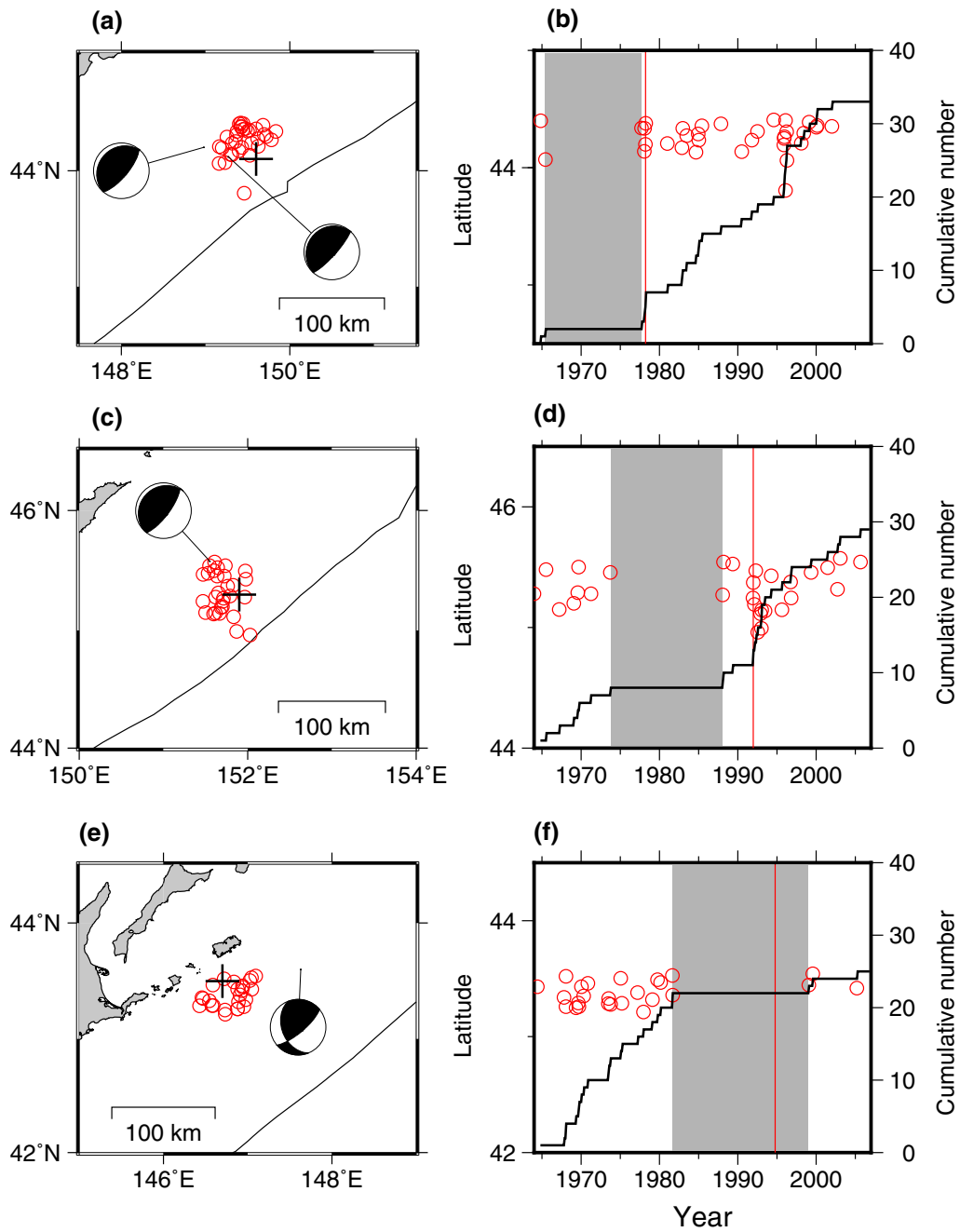


Figure 7

Seismic quiescence areas with $\log_{10}P \leq -4.0$. The node groups close to **a** the 1978 $M_w7.6$ and $M_w7.5$ events, **c** the 1991 $M_w7.6$ event, and **e** the 1994 $M_w8.3$ event. Red circles indicate earthquakes that occurred within the seismic quiescence area, and the center of the area is shown by a cross. The plate boundary is shown by solid lines (Bird 2003). **b**, **d**, and **f** Space–time plot of epicenters within the seismic quiescence area in red circles, and the cumulative number curve is shown by black lines. Vertical red lines indicate the time of occurrence of the main shock

first group is located near the 2006 earthquake, as described above. The second group is located around a node (44.2 °N, 149.4 °E) 14 km east of the centroid

of the 1978 $M_w7.6$ and $M_w7.5$ earthquakes (Fig. 7a, b). The third group is located at a node (45.3 °N, 151.9 °E) 41 km southeast of the centroid of the 1991

M_w 7.6 earthquake (Fig. 7c, d). The fourth group is located around a node (43.5 °N, 146.7 °E) 76 km west of the centroid of the 1994 M_w 8.3 earthquake (Fig. 7e, f). The seismic quiescence usually ends before the main shock; however, in Fig. 7f, it ends after the main shock. This is a natural result of removing aftershocks by a declustering process. Six main shocks within the CI are listed in the Global CMT catalog between 1976 and 2006 with $M_w = 7.5$ or larger and a centroid depth = 100 km or shallower. Good correlation is observed between the seismic quiescence and the six large earthquakes in the study area. However, there is still insufficient evidence of a causal relationship. If causality is not proven, it cannot be concluded that seismic quiescence is a precursor to large earthquakes.

We estimated the probability that the seismic quiescence is observed by chance through conducting a numerical simulation. The numerical simulation is based on a method developed by Zhuang et al. (2004). We produced a simulated earthquake catalog including the background and clustered seismicity in the Kurile Islands region based on the ETAS model with an assumption of the ETAS parameters obtained in this study. An R code used to produce the simulated catalog is presented in supplementary material 5. We applied the declustering process to the simulated catalog and calculated the P -value in the same way as when analyzing a real earthquake catalog. The smallest P -value was searched in the focal area, i.e. 45.5–48.0 °N and 152–156 °E and in the time period between $t = 2005.0$ and 2006.8. The procedure described above was repeated 500 times and made a histogram of the smallest P -value (Fig. 8). In the analysis of the actual earthquake catalog, the smallest P -value at $t = 2005.5$ was $\log_{10}P = -4.05$. In the numerical simulation, the smallest P -value was less than $\log_{10}P = -4.05$ in 20 out of 500 times, i.e. 4%. Therefore, we concluded that the probability of this seismic quiescence being observed by chance is quite low.

6. Conclusions

Katsumata (2017) pointed out that no long-term seismic quiescence was observed before the $M_w =$

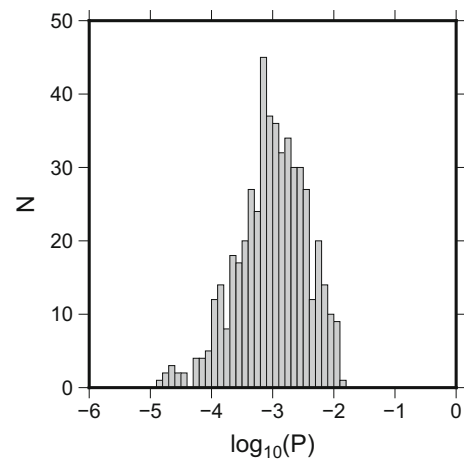


Figure 8

The smallest P -value from a numerical simulation of seismicity based on the ETAS model. During the 500 repetitions, the smallest P -value was estimated in the time period between 2005.0 and 2006.8 in the focal area of the 2006 Kurile Islands earthquake

8.3 Kurile Islands earthquake on 15 November 2006 using the ZMAP method. In the present study, a new method, PMAP, was developed in order to improve on the performance of the ZMAP method, and it was applied to the 2006 earthquake. The seismic quiescence was found to have started at the beginning of 1990, i.e. 16.7 years before the occurrence of the 2006 earthquake, and the seismic quiescence area was located very close to the large asperity ruptured by the 2006 main shock. Thus, seismic quiescence that was not detected by the ZMAP method was detected by the PMAP method, indicating that PMAP is more effective, at least for the 2006 earthquake.

Acknowledgements

We thank two anonymous reviewers and the editor, Benjamin Edwards, for valuable comments. The source code for the program used for the space–time ETAS model and stochastic declustering is available at <https://bemlar.ism.ac.jp/zhuang/software.html>. GMT-SYSTEM (<https://gmt.soest.hawaii.edu/>) version 5.4 (Wessel et al. 2013) was used to create all of the figures in the present study. The present study was supported by the Ministry of Education, Culture, Sports, Science and Technology (MEXT) of Japan

under its Earthquake and Volcano Hazards Observation and Research Program.

Open Access This article is licensed under a Creative Commons Attribution 4.0 International License, which permits use, sharing, adaptation, distribution and reproduction in any medium or format, as long as you give appropriate credit to the original author(s) and the source, provide a link to the Creative Commons licence, and indicate if changes were made. The images or other third party material in this article are included in the article's Creative Commons licence, unless indicated otherwise in a credit line to the material. If material is not included in the article's Creative Commons licence and your intended use is not permitted by statutory regulation or exceeds the permitted use, you will need to obtain permission directly from the copyright holder. To view a copy of this licence, visit <http://creativecommons.org/licenses/by/4.0/>.

Publisher's Note Springer Nature remains neutral with regard to jurisdictional claims in published maps and institutional affiliations.

REFERENCES

- Beck, S. L., & Ruff, L. J. (1987). Rupture process of the great 1963 Kurile Islands earthquake sequence: Asperity interaction and multiple event rupture. *Journal of Geophysical Research*, *92*, 14123–14138.
- Bird, P. (2003). An updated digital model of plate boundaries. *Geochemistry, Geophysics, Geosystems*, *4*(3), 1027.
- Dziewonski, A. M., Chou, T.-A., & Woodhouse, J. H. (1981). Determination of earthquake source parameters from waveform data for studies of global and regional seismicity. *Journal of Geophysical Research*, *86*, 2825–2852.
- Ekström, G., Nettles, M., & Dziewonski, A. M. (2012). The global CMT project 2004–2010: Centroid-moment tensors for 13,017 earthquakes. *Physics of the Earth and Planetary Interior*, *200–201*, 1–9.
- Fedotov, S. A. (1968). The seismic cycle, possibility of the quantitative seismic zoning, and long-term seismic forecasting. In S. V. Medvedev (Ed.), *Seismic Zoning in the USSR* (pp. 133–166). Moscow: Nauka.
- Gardner, J. K., & Knopoff, L. (1974). Is the sequence of earthquakes in Southern California, with aftershocks removed, Poissonian? *Bulletin of Seismological Society of America*, *64*, 1363–1367.
- Gentilia, S., Peresana, A., Talebib, M., Zareb, M., & Giovambattista, R. D. (2019). A seismic quiescence before the 2017 Mw 7.3 Sarpol Zahab (Iran) earthquake: Detection and analysis by improved RTL method. *Physics of the Earth and Planetary Interior*, *290*, 10–19.
- Huang, Q. (2004). Seismicity pattern changes prior to large earthquakes—An approach of the RTL algorithm. *Terrestrial Atmospheric and Oceanic Sciences (TAO)*, *15*, 469–491.
- Inouye, W. (1965). On the seismicity in the epicentral region and its neighborhood before the Niigata earthquake. *Kenshin-jiho (Quarterly Journal of Seismology)*, *29*, 139–144. (in Japanese).
- International Seismological Centre (2013). On-line Bulletin. <https://www.isc.ac.uk> International Seismological Center, Thatcham, United Kingdom.
- Johnson, J. M., & Satake, K. (1999). Asperity distribution of the 1952 great Kamchatka earthquake and its relation to future earthquake potential in Kamchatka. *Pure and Applied Geophysics*, *154*, 541–553.
- Kanamori, H. (1970). Synthesis of long-period surface waves and its application to earthquake source studies—Kurile Islands earthquake of October 13, 1963. *Journal of Geophysical Research*, *75*, 5011–5027.
- Kanamori, H. (1976). Re-examination of the Earth's free oscillations excited by the Kamchatka earthquake of November 4, 1952. *Physics of the Earth and Planetary Interior*, *11*, 216–226.
- Katsumata, K. (2011). Precursory seismic quiescence before the Mw = 8.3 Tokachi-oki, Japan earthquake on 26 September 2003 revealed by a re-examined earthquake catalog. *Journal of Geophysical Research*, *116*, B10307.
- Katsumata, K. (2017). Long-term seismic quiescences and great earthquakes in and around the Japan subduction zone between 1975 and 2012. *Pure and Applied Geophysics*, *174*, 2427–2442.
- Keilis-Borok, V. I., & Kossovokov, V. G. (1990). Premonitory activation of earthquake flow: Algorithm M8. *Physics of the Earth and Planetary Interiors*, *61*, 73–83.
- Kelleher, J., & Savino, J. (1975). Distribution of seismicity before large strike slip and thrust-type earthquakes. *Journal of Geophysical Research*, *80*, 260–271.
- Kelleher, J., & McCann, W. (1976). Buoyant zones, great earthquakes and unstable boundaries of subduction. *Journal of Geophysical Research*, *81*, 4885–4896.
- Lay, T., Kanamori, H., Ammon, C. J., Hutko, A. R., Furlong, K., & Rivera, L. (2009). The 2006–2007 Kuril Islands great earthquake sequence. *Journal of Geophysical Research*, *114*, B11308.
- McCann, W. R., Nishenko, S. P., Sykes, L. R., & Krause, J. (1979). Seismic gaps and plate tectonics: Seismic potential for major boundaries. *Pure and Applied Geophysics*, *117*, 1082–1147.
- Mogi, K. (1969). Some feature of recent seismic activity in and near Japan (2), Activity before and after great earthquakes. *Bulletin of Earthquake Research Institute, University of Tokyo*, *47*, 395–417.
- Nishenko, S. P. (1991). Circum-Pacific seismic potential 1989–1999. *Pure and Applied Geophysics*, *135*, 169–259.
- Ogata, Y. (1988). Statistical model for earthquake occurrences and residual analysis for point processes. *Journal of American Statistical Association*, *83*, 9–27.
- Ogata, Y. (1992). Detection of precursory relative quiescence before great earthquakes through a statistical model. *Journal of Geophysical Research*, *97*, 19845–19871.
- Ogata, Y. (2004). Space-time model for regional seismicity and detection of crustal stress changes. *Journal of Geophysical Research*, *109*, B03308.
- Ohtaka, M., Matsumoto, T., & Latham, G. V. (1977). Seismicity gap near Oaxaca, Southern Mexico as a probable precursor to a large earthquake. *Pure and Applied Geophysics*, *115*, 375–386.
- Seno, T., Sakurai, T., & Stein, S. (1996). Can the Okhotsk plate be discriminated from the North American plate? *Journal of Geophysical Research*, *101*, 11305–11315.

- Sobolev, G. A., & Tyupkin, Y. S. (1997). Low-seismicity precursors of large earthquakes in Kamchatka. *Volcanology and Seismology*, *18*, 433–446.
- Storchak, D. A., Harris, J., Brown, L., Lieser, K., Shumba, B., Verney, R., et al. (2017). Rebuild of the Bulletin of the International Seismological Centre (ISC), part 1: 1964–1979. *Geoscience Letters*, *4*, 32.
- Takahashi, H., Kasahara, M., Kimata, F., Miura, S., Heki, K., Seno, T., et al. (1999). Velocity field of around Sea of Okhotsk and Sea of Japan regions determined from a new continuous GPS network data. *Geophysical Research Letters*, *26*, 2533–2536.
- Utsu, T. (1968). Seismic activity in Hokkaido and its vicinity. *Geophysical Bulletin of Hokkaido University*, *13*, 99–103. (in Japanese).
- Utsu, T. (1969). Some problems of the distribution of earthquakes in time (Part 1). *Geophysical Bulletin of the Hokkaido University*, *22*, 73–93.
- Wessel, P., Smith, W. H. F., Scharroo, R., Luis, J., & Wobbe, F. (2013). Generic mapping tools: Improved version released. *EOS Transaction American Geophysical Union*, *94*(45), 409–410.
- Wiemer, S., & Wyss, M. (1994). Seismic quiescence before the Landers ($M=7.5$) and Big Bare ($M=6.5$) 1992 earthquakes. *Bulletin of the Seismological Society of America*, *84*, 900–916.
- Wiemer, S., & Wyss, M. (2000). Minimum magnitude of completeness in earthquake catalogs: examples from Alaska, the western United States, and Japan. *Bulletin of Seismological Society of America*, *90*, 859–869.
- Wu, Y., & Chiao, L. (2006). Seismic quiescence before the 1999 Chi-Chi, Taiwan, $M_w7.6$, earthquake. *Bulletin of the Seismological Society of America*, *96*, 321–327.
- Wyss, M., & Habermann, R. E. (1979). Seismic quiescence precursory to a past and a future Kurile Island earthquake. *Pure and Applied Geophysics*, *117*, 1195–1211.
- Wyss, M., Hasegawa, A., Wiemer, S., & Umino, N. (1999). Quantitative mapping of precursory seismic quiescence before the 1989, $M7.1$ off-Sanriku earthquake, Japan. *Annali di Geofisica*, *42*, 851–869.
- Zhuang, J., Ogata, Y., & Vere-Jones, D. (2004). Analyzing earthquake clustering features by using stochastic reconstruction. *Journal of Geophysical Research*, *109*, B05301. <https://doi.org/10.1029/2003JB002879>.
- Zhuang, J., Chang, C.-P., Ogata, Y., & Chen, Y.-I. (2005). A study on the background and clustering seismicity in the Taiwan region by using point process models. *Journal of Geophysical Research*, *110*, B05S18.

(Received June 25, 2019, revised December 10, 2019, accepted April 27, 2020, Published online May 8, 2020)